

DOI: 10.1002/adma.200602966

## Structure-Dependent Electrical Properties of Carbon Nanotube Fibers\*\*

By Qingwen Li, Yuan Li, Xiefei Zhang, Satishkumar B. Chikkannanavar, Yonghao Zhao, Andrea M. Dangelewicz, Lianxi Zheng, Stephen K. Doorn, Quanxi Jia, Dean E. Peterson, Paul N. Arendt, and Yuntian Zhu\*

Spun carbon nanotube (CNT) fibers have great potential for conducting and sensing applications owing to their unique, tunable electrical properties.<sup>[1–5]</sup> Here we report the electron transport properties of neat, well-aligned CNT fibers spun from arrays of millimeter-long CNTs. The conductivity of as-spun CNT fibers is around  $595.2 \text{ S cm}^{-1}$  at room temperature, and its variation with temperature shows a semiconductive behavior from 300 to 75.4 K. The electron transport was found to follow a three-dimensional (3D) hopping mechanism.<sup>[6]</sup> Importantly, it was found that chemical treatments may significantly affect the conductivities of as-spun fibers. Oxidizing the CNT fibers in air or  $\text{HNO}_3$  increased the conductivities, while covalent bonding of Au nanoparticles to the CNT fibers remarkably improved conductivity and changed conduction behavior. Conversely, annealing CNT fibers in  $\text{Ar} + 6\% \text{ H}_2$  at  $800^\circ\text{C}$  or under the CNT array growth conditions at  $750^\circ\text{C}$  led to a dramatic decrease in conductivity.

Owing to their conjugated and highly anisotropic 1D structures, carbon nanotubes (CNTs) are a fascinating new class of electronic materials from both theoretical and applied standpoints.<sup>[7]</sup> The excellent conductivities of CNTs and their ability to carry very high current density, along with their high thermal conductivity, chemical stability, and mechanical strength, make CNTs uniquely promising for a broad range of applications, including building blocks for nanoscale electronic devices, microsensors for bio-agents and chemicals, and power cables for space shuttles.<sup>[8–10]</sup> The electrical resistivity  $\rho$  of individual CNTs has been measured under ballistic conduction to be as low as  $10^{-6} \Omega \text{ cm}^{[11,12]}$  for single-walled and

$3 \times 10^{-5} \Omega \text{ cm}^{[13,14]}$  for multiwalled CNTs, respectively, indicating that CNTs may be better conductors than metals such as copper at room temperature. However, in most cases, due to the presence of various defects or impurities formed during the CNT growth, the conductivities of individual CNTs are often much lower than those under ballistic conduction with nanotubes free of defects.<sup>[15,16]</sup>

The electron transport in CNT assemblies is different from that in individual nanotubes. It has been reported that single-walled carbon nanotube (SWNT) fibers, either synthesized directly by vertical floating chemical vapor deposition (CVD) methods<sup>[1,2]</sup> or extruded from a super-acid suspension,<sup>[3]</sup> exhibit room-temperature resistivities in the range of  $1 \times 10^{-4}$  to  $7 \times 10^{-4} \Omega \text{ cm}$ , which is nearly 100 times higher than the resistivities of single nanotubes. The resistivities of multiwalled carbon nanotube (MWNT) fibers are typically one or two orders of magnitude higher than that of SWNT fibers.<sup>[4,5]</sup> Such large differences between single nanotubes and fiber assemblies may arise from a high impurity content (such as amorphous carbon and catalytic particles) in the fibers, which may profoundly affect electron transport by causing significant scattering, and contact resistances between nanotubes.

Therefore, two approaches can be used to improve the electrical conductivity of CNT fibers: 1) minimize the contact resistances between nanotubes by improving the alignment of CNTs and by increasing the lengths of individual tubes; 2) improve the conductivity of individual CNTs by post-synthesis treatments. It was the objective of the study reported here to use these two approaches to produce CNT fibers with high conductivity and to study the fundamental conduction mechanisms of the CNT fibers.

Thin and clean CNT fibers (typically  $3 \mu\text{m}$  in diameter) were spun from arrays of well-aligned, millimeter-long CNTs, which were synthesized using ethylene CVD on a Fe catalyst film.<sup>[17]</sup> By measuring the resistance of CNT fibers at temperatures from 300 K to 75.4 K, we investigated the electronic properties of as-spun fibers and their possible conducting mechanisms. It was also found that the conductivity of CNT fibers could be tuned through mild post-treatments.

The spun CNT fibers were post-treated with five different procedures: 1) Annealing in air at  $480^\circ\text{C}$  for half an hour in an attempt to clean off the amorphous carbon, whose oxidation temperature is often around  $400^\circ\text{C}$ .<sup>[18]</sup> 2) Oxidizing in dilute  $5 \text{ M HNO}_3$  solution at  $40^\circ\text{C}$  to cause a weak chemical

[\*] Dr. Y. T. Zhu, Dr. Q. W. Li, Y. Li, Dr. X. F. Zhang, Dr. S. B. Chikkannanavar, Dr. Y. H. Zhao, A. M. Dangelewicz, Dr. L. X. Zheng, Dr. S. K. Doorn, Dr. Q. X. Jia, Dr. D. E. Peterson, Dr. P. N. Arendt  
Los Alamos National Laboratory  
Los Alamos, NM 87545 (USA)  
E-mail: yzhu@lanl.gov

[\*\*] This work was supported by the Laboratory Directed Research and Development (LDRD) program office of Los Alamos National Laboratory. We thank Dr. Honghui Zhou for her help in electrical measurements. Supporting Information is available online from Wiley InterScience or from the authors.

functionalization.<sup>[19,20]</sup> 3) Annealing in Ar + 6% H<sub>2</sub> atmosphere at 800 °C to saturate the defective structures.<sup>[21]</sup> 4) Introducing metallic gold nanoparticles onto CNTs by dipping fibers functionalized by 5 M HNO<sub>3</sub> into a 0.01% HAuCl<sub>4</sub> ethanol solution for 5 min.<sup>[22]</sup> 5) Introducing carbon particles by a repeated treatment of the fibers under CNT array growth conditions.<sup>[23]</sup> All of these treatments were chosen to introduce mild modifications to the CNT fibers so that their pristine structures could be maintained while their electrical properties were modified.

Figure 1A shows a typical uniform CNT fiber spun from an array of millimeter-long CNTs. Owing to the thin Fe catalyst used in its synthesis, the catalyst contamination in our CNT arrays is much less than in CNT fibers synthesized by the floating CVD method<sup>[1,2]</sup> and CNT arrays grown on thick Fe films.<sup>[3,4,24,25]</sup> Moreover, CNTs also align very well in our spun fibers, as they can only be spun from super-aligned CNT arrays.<sup>[24,25]</sup> Our spun CNT fibers have good CNT alignment and high purity<sup>[17]</sup> and therefore may serve as a good model system to investigate the electrical properties of CNT assemblies. The inset in Figure 1A reveals that the CNTs are multiwalled (2–7 walls) with an average diameter of 7 nm and that they are more defective than SWNTs and graphite.<sup>[26]</sup> This is evident from the Raman spectrum shown in Figure 1B, where the intensity of the D peak is higher than that of the G peak.

Figure 2 shows the temperature dependence of the resistivity  $\rho$  and conductivity  $\sigma$  of a CNT fiber between 75.4 and 300 K. The resistivity decreases monotonically and smoothly from  $2.19 \times 10^{-3} \Omega \text{ cm}$  at 75.4 K to  $1.68 \times 10^{-3} \Omega \text{ cm}$  at 300 K. Conversely, the conductivity increases with increasing temperature, from  $456.6 \text{ S cm}^{-1}$  at 75.4 K to  $595.2 \text{ S cm}^{-1}$  at 300 K, indicating a semiconducting behavior, but with much smaller temperature dependence than commercial graphite and carbon fibers.<sup>[27]</sup> Under the same synthesis and spinning conditions except for the growth time, the CNT fibers spun from an array of 0.3 mm long CNTs showed a conductivity of

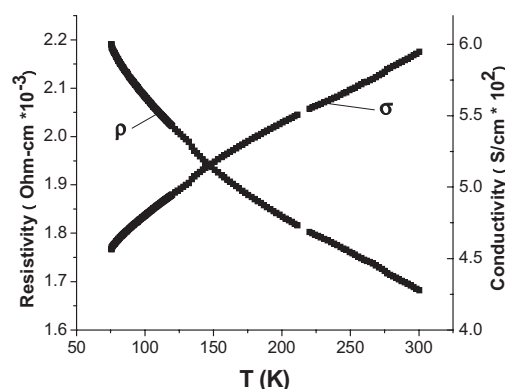


**Figure 2.** Temperature dependence of the resistivity ( $\rho$ ) and conductivity ( $\sigma$ ) of a spun CNT fiber.

$465.3 \text{ S cm}^{-1}$  at 300 K, which is about 22% lower than the fiber from an array of 1.0 mm CNTs. This indicates that CNT fibers spun from arrays of longer CNTs will have lower contact resistance. This is likely due to the fact that a fiber made of longer CNTs will have fewer end connections and larger contact area between neighboring tubes. For a given specific contact resistance, the larger the contact area, the smaller the total contact resistance. As a result, our CNT fiber is more conductive than other reported CNT fibers, its conductivity being at least 49.5% higher than those reported previously.<sup>[3,4]</sup>

The temperature dependence of conductivity can help with understanding the conduction mechanism of a CNT fiber. Unlike that of a single tube, the resistivity of a CNT fiber is derived from two components: the resistance of individual CNTs and the contact resistance between CNTs. As mentioned above, the resistivities of individual tubes are often two orders of magnitude lower than their assemblies,<sup>[3,4]</sup> which suggests

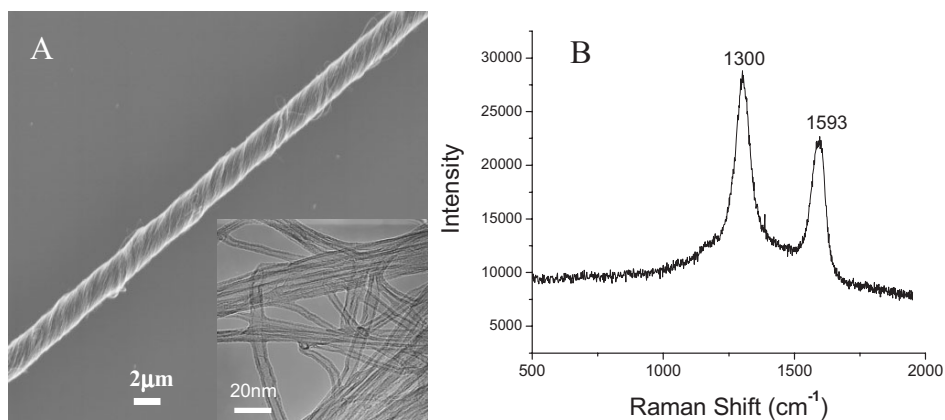


**Figure 1.** A) Scanning electron microscopy (SEM) image of a spun CNT fiber; the typical diameter of the fiber used in the study is 3  $\mu\text{m}$ . Inset: Transmission electron microscopy (TEM) image showing CNTs are multiwalled with an average diameter of 7 nm. B) Raman spectrum of the spun fiber, revealing a highly defective structure formed in the CNTs.

that the contact resistances at the interfacial connections of CNTs play a significant role in the conduction behavior of a CNT fiber. In general, two main mechanisms can be used to explain the conduction behavior of semiconductive CNTs: variable range hopping (VRH)<sup>[28]</sup> and tunneling conduction (TC).<sup>[29]</sup> They can be described with the following two equations, respectively:

$$\sigma T^{1/2} = \exp(-B/T^{1/4}) \quad (1)$$

$$\sigma = \sigma_0 \exp(-A/T^{1/2}) \quad (2)$$

where  $\sigma$  is the electrical conductivity,  $\sigma_0$ ,  $A$ , and  $B$  are constants, and  $T$  is absolute temperature. As shown in Figure 3, plotting our data in the form  $\ln(\sigma T^{1/2})$  versus  $T^{-1/4}$ , based on Equation 1, gives a much more linear plot than  $\ln \sigma$  versus  $T^{-1/2}$ , based on Equation 2, which indicates that the conduction in our spun fibers is predominantly controlled by the hopping mechanism. The slight deviation from the straight line in Figure 3A at high temperatures was probably caused by electron tunneling between some CNTs.

In more detail, the relationship between conductivity and temperature in Mott's variable range hopping model can also be expressed as  $\sigma \propto \exp(-A/T^{1/(d+1)})$ , where  $A$  is a constant and  $d$  is the dimensionality.<sup>[6]</sup> The plot of  $\ln \sigma$  versus  $T^{-1/4}$  (for  $d=3$ ),  $T^{-1/3}$  (for  $d=2$ ), and  $T^{-1/2}$  (for  $d=1$ ) have linear fitting coefficients of 0.997, 0.995, and 0.992, respectively. This suggests that the electron transport in CNT fibers is consistent with a 3D hopping mechanism. This behavior is most likely due to the defect structures of CNTs, in which electrons cannot be confined in the 1D channels of CNTs, and instead hop from one localized site to another, or possibly from one CNT to another. The energy difference be-

tween the initial and final states is bridged by an electron-phonon scattering process.<sup>[30]</sup>

The two-terminal current-voltage ( $I$ - $V$ ) characteristics of a spun CNT fiber (shown in Fig. S2, Supporting Information) indicate a linear nature of the  $I$ - $V$  curve, which reveals good ohmic contacts between the CNT fiber and the electrodes. The resistance  $R$  as derived from the linear  $I$ - $V$  curve is  $2.2 \times 10^3 \Omega$ , based on  $R = \rho L/S$ , where the length  $L$  is 1 mm and the area  $S$  is  $7.1 \times 10^{-12} \text{ m}^2$  for a CNT fiber with diameter of 3  $\mu\text{m}$ . The corresponding resistivity is calculated to be  $1.56 \times 10^{-3} \Omega \text{ cm}$ , which is consistent with the four-probe measurement.

The conductivities of the CNT fibers changed after different post-synthesis treatments. As shown in Table 1, oxidizing the CNT fiber in both air and  $\text{HNO}_3$  led to an increase in conductivity. Treating the CNT fiber under high temperature in forming gas (Ar+6%  $\text{H}_2$ ) led to a dramatic decrease in its conductivity. Also, annealing the CNT fiber under regrowth conditions (containing hydrogen as well), dramatically decreased its conductivity although some new CNTs were formed on the fiber (shown in Fig. 4A). Among the five treatments, covalently coating gold nanoparticles onto the fiber led to the greatest increase in conductivity. As seen from Figure 4B, although such coating was sparse,

**Table 1.** Effects of chemical treatments on the structures and electrical properties of CNT fibers.

Sample	Conductivity at 75.4 K [ $\text{S cm}^{-1}$ ]	Conductivity at 300K [ $\text{S cm}^{-1}$ ]	D peak position [ $\text{cm}^{-1}$ ]	G peak position [ $\text{cm}^{-1}$ ]	$I_G/I_D$
Original fiber	456.6	595.2	1300	1593	0.67
Annealed in air at 480 °C	642.7	818.3	1300	1598	0.54
Annealed in Ar + 6% $\text{H}_2$ at 800 °C	29.3	70.0	1300	1598	0.48
Oxidized in 5N $\text{HNO}_3$	692.5	969.0	1300	1594	0.41
Coated with Au nanoparticles	907.4	1152.7	1305	1598	0.52
Re-growth at 750 °C	55.3	71.1	1300	1583	0.62

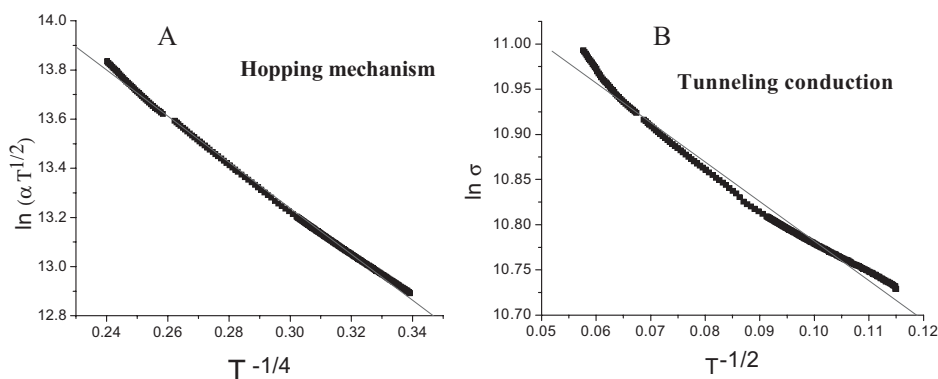


**Figure 3.** Fitting of the conductivity data of our CNT fibers with two different conduction mechanisms. A) Plot of  $\ln(\sigma T^{1/2})$  versus  $T^{-1/4}$ , based on the variable range hopping (VRH) mechanism. B) Plot of  $\ln \sigma$  versus  $T^{-1/2}$ , based on the tunneling conduction (TC) mechanism.

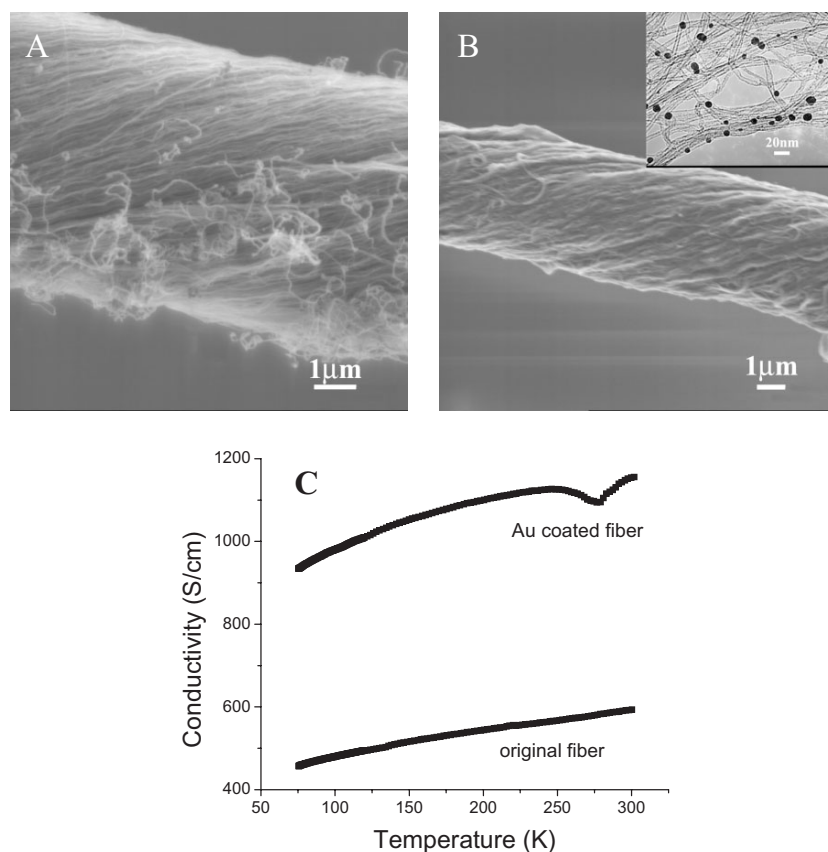


**Figure 4.** A) SEM image of the CNT fiber treated under regrowth conditions, some new nanotubes were found growing on the fiber. B) SEM image of the CNT fiber coated with Au nanoparticles. Inset: TEM image showing that gold nanoparticles were formed sparsely on the nanotubes. C) Comparison of the conductivity temperature dependence between the pure CNT fiber and Au-coated fiber.

Au-coated fiber showed the best conductivity of  $1150 \text{ S cm}^{-1}$ , which is much higher than those of commercial carbon ( $285 \text{ S cm}^{-1}$ )<sup>[31]</sup> and carbon fiber ( $560 \text{ S cm}^{-1}$ ).<sup>[27]</sup> It appears that simple and moderate chemical treatments of the as-spun CNT fibers result in remarkable improvement in electrical conductivity.

Except for the Au-coated fiber, all treated CNT fibers showed a conductivity increase with temperature over the entire temperature range from 75 K to 300 K. In contrast, as shown in Figure 4C, the Au-coated fiber exhibited a unique conductivity–temperature relationship. At temperatures below 250 K, the conductivity increased with temperature, indicating a semiconductive nature. At temperatures higher than 250 K, the conductive behavior changed to metallic, but then switched back to semiconductive when temperatures were above 280 K. Such conductivity fluctuations were also observed in DNA-linked Au nanoparticle aggregates<sup>[32]</sup> and Au composites,<sup>[33]</sup> implying that Au nanoparticles play an important role in the conducting behavior of the fiber at higher temperatures but the conductance at lower temperatures is dominated by CNTs.

The changes of the electrical properties of CNT fibers can be related to their structural modifications,<sup>[34]</sup> which were elucidated using Raman spectroscopy. The content and types of defects in the CNTs treated using different routes were evaluated based on the locations of the D and G peaks, and the ratio  $I_G/I_D$ .<sup>[35]</sup> In a typical Raman spectrum of CNTs, the D peak is located between  $1330$  and  $1360 \text{ cm}^{-1}$  and is assigned to disordered carbon (defects and amorphous carbon), while the G peak is around  $1580 \text{ cm}^{-1}$  and corresponds to the stretching mode in the graphene plane. As shown in Table 1, except for the regrowth route, all treatments led to an obvious decrease of  $I_G/I_D$ , suggesting that CNTs become more defective after these treatments.

Interestingly, annealing CNT fibers in air at  $480^\circ\text{C}$  did not reduce the  $I_D$  peak, but resulted in an  $I_G/I_D$  ratio even lower than that of the as-spun fiber. As amorphous carbon is reported to start burning at  $300^\circ\text{C}$ ,<sup>[18]</sup> the increase of the  $I_D$  peak instead of a decrease after heat treatment indicates that the contribution of the defective  $\text{sp}^2$  carbon to the D peak is dominant in the present case. Burning the fiber sample in air at around  $480^\circ\text{C}$  enabled the defective carbons to be functionalized into carboxylic groups (COOH),<sup>[19,36]</sup> leading to a higher D peak and a shift in its G peak.

Refluxing CNTs in dilute  $\text{HNO}_3$  has been reported to yield etched carbonaceous particles and to functionalize defect sites of CNTs into carboxylic groups.<sup>[19]</sup> Our experiments indicate that oxidizing the CNT sample in 5 M  $\text{HNO}_3$  causes more severe damage to CNTs than oxidation in air. This also showed the lowest  $I_G/I_D$  of the five treatments, indicating that more defect sites were formed on nanotubes under these conditions where CNTs were functionalized with C=O groups.

As shown in Figure 4B, dipping an acid-treated fiber into a 0.01%  $\text{H}_4\text{AuCl}_3$  solution spontaneously, but not densely, deposits gold nanoparticles onto the side walls of nanotubes without the assistance of any other reducing reagent. This kind of reaction can only occur on functionalized nanotubes.<sup>[37]</sup> The result in Figure 4B also indicates that the functionalization efficiency in 5 M  $\text{HNO}_3$  is low, and gold nanoparticles with an average size around 10 nm were sparsely distributed on the nanotubes.

Annealing the as-spun CNT fiber in hydrogen atmosphere (Ar + 6%  $\text{H}_2$ ) at a high temperature also resulted in obvious

damage to the nanotube structures. An increase of the D peak and a red shift of the G peak suggest that the presence of hydrogen at high temperatures may help to reduce defective sp<sup>2</sup> bonds (C=C) into saturated sp<sup>3</sup> bonds (C-H).<sup>[38]</sup> Treating the CNT fiber under regrowth conditions including a hydrogen atmosphere leads to the formation of some small CNTs on the fiber, but with a drop in  $I_G/I_D$  as well.

The dependence of conductivity of CNT fibers on their structures can be attributed to the variation in carrier density and  $\pi$ -bonding system of CNTs caused by different chemical treatments. Both as-spun and treated CNT fibers show a conductivity increase at low temperatures, suggesting that the carrier density increased with temperature. When CNT fibers are functionalized with carboxylic groups, where the  $\pi$ -conjugated system of CNTs can be maintained, the CNTs are doped by the acceptor dopant groups. As a result, the conductivity of the fibers is enhanced due to an increase in carrier density.<sup>[34]</sup> In contrast, the covalent coating of metallic Au nanoparticles onto CNTs appears to further increase carrier density, leading to an obvious increase in conductivity. Conversely, the formation of sp<sup>3</sup> bonds in CNTs during annealing in hydrogen-containing atmosphere at high temperatures may interrupt the planar  $\pi$ -conjugated structure of CNTs, causing a severe disruption of the electron transport in CNTs and therefore a sharp decrease of the conductivity.<sup>[38,39]</sup>

In summary, CNT fibers spun from arrays of millimeter-long CNTs are composed of clean and well-aligned CNTs. Their conductive behavior indicates that they are semiconducting in the temperature range from 75 K to 300 K. Furthermore, they show better conductivity than commercial carbon, carbon fiber, and previously reported CNT fibers. The conduction of the as-spun CNT fiber fits the  $T^{-1/4}$  hopping law very well, indicating that electrons conduct along the CNT fiber by a 3D hopping mechanism. The carrier density seems to play an important role in their conduction behavior.

The electrical properties of CNT fibers are largely dependent on structural changes caused by different chemical treatments. Introduction of acceptor dopants into CNT conjugated systems by oxidizing CNTs in air or HNO<sub>3</sub> helps to increase the conductivity of CNT fibers, while annealing CNTs in a hydrogen-containing atmosphere may significantly lower their conductivity due to the formation of sp<sup>3</sup> carbon bonds. Covalent coating of Au nanoparticles onto the CNTs not only significantly enhances conductivity, but also changes the conducting mechanism. These results provide insight into the electron transport behavior in the  $\pi$ -conjugated CNT system, and useful strategies to manipulate the electronic properties of CNTs for potential applications in electronics, sensing, and conducting wires.

## Experimental

Arrays of millimeter-long CNTs were synthesized at 750 °C with 100 sccm ethylene and 100 sccm forming gas for 15 min. The CNT fibers were spun from CNT arrays with a spindle rotating at 2500 rpm

and drawing at 5 cm min<sup>-1</sup>. The diameters of the spun fibers were measured using scanning electron microscopy (SEM).

Electrical measurements were conducted using the four-probe method at temperatures from 75.4 K to 300 K with a sampling interval of 0.02 K. The constant direct current passing through the fiber was set at 10  $\mu$ A. In order to build up a good contact between the thin fiber and the electrode, a prepatterned glass substrate with four Pt electrode strips was made using sputtering through a shadow mask. The four Pt strips were 300 nm thick, 1 mm wide, 5 mm long, and separated by 1 mm. The fibers were transferred onto the prepatterned substrates. As illustrated in Figure S1, a thin layer of silver paste covered the fiber at each Pt electrode.

Received: December 27, 2006

Revised: May 25, 2007

Published online: September 20, 2007

- [1] H. W. Zhu, L. Xu, D. Wu, B. Q. Wei, R. Vajtai, P. M. Ajayan, *Science* **2002**, *296*, 884.
- [2] Y. Li, I. A. Kinloch, A. H. Windle, *Science* **2004**, *304*, 276.
- [3] W. Zhou, J. Vavro, C. Guthy, K. I. Winey, J. E. Fisher, R. E. Smalley, *J. Appl. Phys.* **2004**, *95*, 649.
- [4] M. Zhang, K. R. Atkinson, R. H. Baughman, *Science* **2004**, *306*, 1358.
- [5] L. Zhu, J. Xu, Y. Xiu, W. H. Hess, C. P. Wong, *Carbon* **2006**, *44*, 253.
- [6] S. N. Mott, *Conduction in Non-crystalline Materials*, Clarendon, Oxford **1987**.
- [7] R. H. Baughman, A. A. Zakhidov, W. A. de Heer, *Science* **2002**, *297*, 787.
- [8] P. L. McEuen, J. Park, *MRS Bull.* **2004**, *29*, 272.
- [9] A. P. Ramirez, *Bell Labs Tech. J.* **2005**, *10*, 171.
- [10] H. J. Dai, *Acc. Chem. Res.* **2002**, *35*, 1035.
- [11] P. L. McEuen, M. Fuhrer, H. Park, *IEEE Trans. Nanotechnol.* **2002**, *2*, 78.
- [12] B. Gao, Y. F. Chen, M. S. Fuhrer, D. C. Glattli, A. Bachtold, *Phys. Rev. Lett.* **2005**, *95*, 196802.
- [13] A. Bachtold, M. Henny, C. Terrier, C. Strunk, L. Forro, *Appl. Phys. Lett.* **1998**, *73*, 274.
- [14] C. Berger, Y. Yi, Z. L. Wang, W. A. de Heer, *Appl. Phys. A* **2002**, *74*, 363.
- [15] S. N. Song, X. K. Wang, R. P. Chang, J. B. Ketterson, *Phys. Rev. Lett.* **1994**, *72*, 697.
- [16] H. J. Dai, E. W. Wong, C. M. Lieber, *Science* **1996**, *272*, 523.
- [17] Q. W. Li, X. F. Zhang, R. F. DePaula, L. X. Zheng, Y. H. Zhao, L. Stan, T. G. Holesinger, P. N. Arendt, D. E. Peterson, Y. T. Zhu, *Adv. Mater.* **2006**, *18*, 3160.
- [18] R. Sen, S. M. Richard, M. E. Itkis, R. C. Haddon, *Chem. Mater.* **2003**, *15*, 4273.
- [19] J. Zhang, H. Zou, Q. Qing, Y. Yang, Q. Li, Z. Liu, *J. Phys. Chem. B* **2003**, *107*, 3712.
- [20] S. Niyogi, M. A. Hamon, H. Hu, B. Zhao, P. Bhowmik, R. Sen, M. E. Itkis, R. C. Haddon, *Acc. Chem. Res.* **2002**, *35*, 1105.
- [21] S. R. C. Vivekchand, A. Govindaraj, Md. Motin Seikh, C. N. R. Rao, *J. Phys. Chem. B* **2004**, *108*, 6935.
- [22] H. C. Choi, M. Shim, S. Bangsaruntip, H. Dai, *J. Am. Chem. Soc.* **2002**, *124*, 9058.
- [23] Z. Zhu, Y. Lu, D. Qiao, S. Bai, T. Hu, L. Li, J. Zheng, *J. Am. Chem. Soc.* **2005**, *127*, 15698.
- [24] X. B. Zhang, K. L. Jiang, C. Feng, P. Liu, S. S. Fan, *Adv. Mater.* **2006**, *8*, 1505.
- [25] K. L. Jiang, Q. Li, S. S. Fan, *Nature* **2002**, *419*, 801.
- [26] H. Hinra, T. W. Ebbesen, K. Tanigaki, T. Takahashi, *Chem. Phys. Lett.* **1993**, *202*, 509.
- [27] D. D. L. Chung, *Carbon Fiber Composites*, Butterworth-Heinemann, Newton, MA **1994**, Ch. 2.

- [28] H. R. Zeller, *Phys. Rev. Lett.* **1972**, *28*, 1452.
- [29] M. F. Matare, *J. Appl. Phys.* **1984**, *56*, 2605.
- [30] C. H. Jin, J. Y. Wang, Q. Chen, L. M. Peng, *J. Phys. Chem. B* **2006**, *110*, 5423.
- [31] J. D. Cutnell, K. W. Johnson, *Physics*, 7th ed., Wiley, New York **2006**, Ch. 20.
- [32] Y. J. Yun, G. Park, S. Jung, D. H. Ha, *Appl. Phys. Lett.* **2006**, *88*, 063 902.
- [33] A. A. Babaev, I. K. Kamilov, S. B. Sultanov, A. M. Askhabov, P. P. Khokhlachec, *J. Optoelectron. Adv. Mater.* **2005**, *7*, 2013.
- [34] A. Skakalova, A. B. Kaiser, U. Dettlaff-Weglikowska, S. Roth, *J. Phys. Chem. B* **2005**, *109*, 7174.
- [35] A. Jorio, M. A. Pimenta<sup>1</sup>, A. G. Souza Filho, R. Saito, G. Dresselhaus, M. S. Dresselhaus, *New J. Phys.* **2003**, *5*, 139.
- [36] Q. Li, J. Zhang, Z. F. Liu, *J. Phys. Chem. B* **2002**, *106*, 11 085.
- [37] X. Xu, T. Wang, X. Qu, S. Dong, *J. Phys. Chem. B* **2006**, *110*, 853.
- [38] G. Zhang, P. Qi, X. Wang, Y. Lu, D. Mann, H. Dai, *J. Am. Chem. Soc.* **2006**, *128*, 6026.
- [39] H. Park, J. Zhao, J. P. Lu, *Nano Lett.* **2006**, *6*, 916.